Whale Optimization Algorithm for Ship Path Optimization in Large-Scale Complex Marine Environment

QILONG HAN [ID], XIAO YANG [ID], HONGTAO SONG, SHANSHAN SUI, HUI ZHANG, AND ZAIQIANG YANG

College of Computer Science and Technology, Harbin Engineering University, Harbin 150001, China

Corresponding author: Hongtao Song (songhongtao@hrbeu.edu.cn)

ABSTRACT With the formulation of United Nations Convention on the Law of the Sea, marine pollution has received widespread attention from various countries. Green navigation is an important requirement for route planning, in which energy consumption is its primary focus. Ships are affected by complex marine meteorological environments, so it is difficult to plan a reasonable route. Some methods have been proposed to solve this problem, but there are some shortcomings, such as no consideration of the effect of wind direction, wind speed and wave. To solve this problem, we introduce a meta-heuristic whale optimization algorithm (WOA), which helps ships find a low-energy-consumption and safe route in a large-scale complex marine environment. The results of our simulation experiments indicate that WOA is more competitive than other state-of-the-art algorithms for route planning.

INDEX TERMS Marine pollution, marine meteorological, meta-heuristic, whale optimization algorithm.

I. INTRODUCTION

The movement of ships is affected by various marine environmental disturbances, such as wind and waves. In particular, due to the complexity and variability of marine meteorology in oceantransportation, the ship's navigation needs to be adjusted in time according to different time and latitude and longitude weather information. Therefore, when designing a ship's navigation path or a set of route points, it is necessary to consider the impact of the marine climate and improve navigation efficiency. There is a economically feasible path to be generated when the navigation time is satisfied. In addition, the ship is an under-actuated system, and its degree of freedom of movement is higher than the number of its driving modes. The motion of an underdriven vehicle is limited by the vehicle's inherent motion constraints, so it is important to generate a feasible path for a vehicle with these motion characteristics [1].

The associate editor coordinating the review of this manuscript and approving it for publication was Eklas Hossain [ID].

Marine meteorology is closely related to navigational activities, especially wind speed and waves, which are often in constant or even severe movements. The influence of marine meteorological conditions on navigation is very important. In addition to stalling or increasing the wind speed, the ship drifted downwind on the one hand and deflected the ship on the other. Due to the different wind characteristics of the stable wind and the sudden wind, the wind direction sometimes changes, and the relative wind direction of the ship also changes when the ship turns. When the draft is different, the wind receiving area will also be very different [2]. Facing the harsh environment of strong winds and waves, the operator needs to adjust the course in time, adjust the ship's trim, and choose the appropriate anchoring area. This adds to the complexity of ship maneuvering. When a ship sails in a high wind and wave area, the ship will experience more severe sway motion, speed reduction, unstable course, and other manipulation difficulties caused by it [3]. The establishment of the route is mainly based on the latest weather conditions and a large amount of sea state data. Wind speed and wave height change dynamically along with time and geographical location. In order to optimize the route, it is

necessary to consider these dynamic changes and the sailing conditions of the ship. According to the European Center for Medium-Term Weather Forecasting, we can obtain marine meteorological information at each latitude and longitude at different times.Our purpose is to find the best path meeting ship navigation constraints under complex marine weather, that is, to find a route between the origin and destination, which can ensure that the ship is the most economical under certain constraints.

However, due to the limitation of current technology, the latest ship path technology only considers the marine conditions only in small-scale areas or fixed areas. In the face of large-scale complex marine environment, it is difficult to use traditional optimization methods, such as Newton's method, conjugate gradient method, Powell method, Lagrangian multiplier method, branch and bound method, and dynamic programming method [4]. In the large-scale complex marine environment, the wind speed and wave height for each latitude and longitude are different, so it is difficult to give a feasible solution in a reasonable time. Therefore, it is extremely important to find a novel large-scale optimization method to solve these real-world large-scale and complex problems. In recent years, meta-heuristic algorithms have received widespread attention from scholars [5]. The main purpose of the development of meta-heuristic algorithms is to quickly solve path planning problem and get satisfactory solutions. The meta-heuristic algorithm has exhibited good performance in solving most of the nonlinear and multimodal practical optimization problems [6]. At the same time, it has also been widely used, such as dynamic optimization, infinite impulse response filter design, image processing, mechanical design issues, task scheduling, data mining and other engineering issues. Its superior energy comes from studying the laws of physical, social and biological phenomena in nature, and imitating the best characteristics of natural phenomena.

Whale Optimization Algorithm (WOA) is a new swarm intelligence optimization method proposed by Mirjalili [7]. This idea is derived from the special predatory behavior unique to humpback whales in the ocean. The whale optimization algorithm achieves the optimization goal through the simulation of whale rounding, bubble attack and search behavior. The algorithm has the characteristics of simple principle, simple operation, easy implementation, few parameters to be adjusted and strong robustness. In terms of function optimization, the WOA is significantly superior to algorithms such as particle swarm optimization (PSO) [8], differential evolution (DE) [9] and gravitational search (GSA) [10] in terms of accuracy and stability. At the same time, the WOA has been widely used in many fields, such as economic dispatch, photovoltaic MPP system, capacitor location and image segmentation.

In recent years, many scholars have proposed some swarm intelligence algorithms to solve path planning problems. Wei proposed swarm hyper-heuristic algorithm to solve path planning of AUV [6]. Ma proposed an improved ant

TABLE 1. Ship parameters.

Ship form parameters	Value
$L_{pp}(m)$	176
$L_{WL}(m)$	179.995
$B(m)$	32.2
$T(m)$	11
$T1(m)$	20
C_b	0.85
C_P	0.83
$P(m^3)$	50250.8
L_{bp}	2.897
Whether the ship is fully loaded	Fully loaded
F_r	0.184
S	8579.049282
$\rho(Kg/m^3)$	1025
$V_1(kn)$	15.7

colony algorithm based on particle swarm algorithm for path planning of autonomous underwater vehicles [11]. Zamuda proposed difference algorithm for underwater glider path planning [12]. Zhou and Wang proposed an improved flower pollination algorithm (FPA) for path planning of underwater vehicles [13]. Dewangan used gray wolf optimization algorithm to solve 3D path planning [14]. However,no whale optimization algorithm has been proposed to solve the problem of ship path planning under large-scale complex marine weather.

The rest of our paper is structured as follows. In section 2, the path planning of ship model under complicated marine weather is introduced in detail. In section 3, we mainly discuss the principles of whale optimization algorithm in route planning. In section 4, we analysis the simulation experiments. Finally, we summarizes the full paper and proposes future research directions in section 5.

II. THE PATH PLANNING OF SHIP MODEL UNDER COMPLICATED MARINE WEATHER

Different types of ships have different sailing conditions such as drainage and steering. In this paper, the value of drainage is 50250.8. The range of steering is 0° to 35°. Other detailed parameters are given in Table 1. In a large-scale and complicated marine meteorological environment, the ship's path planning model not only needs to meet the constraints of the ship's own conditions, but also needs to consider the impact of marine meteorology on the ship's navigation [15]. We will constrain the ship from the following aspects.

In large-scale and complicated marine weather, many factors affect the navigation route of ships, the most important of which are the resistance of water, the resistance of wind and the influence of waves. This section details the ship path model for a given case under the influence of complex weather.

A. HYDROSTATIC RESISTANCE MODEL

During navigation, the greater the resistance, the greater the power required to meet a certain speed [16]. Similarly, the greater the resistance of the still water during the sailing of a ship, the more power the ship needs, which leads to an
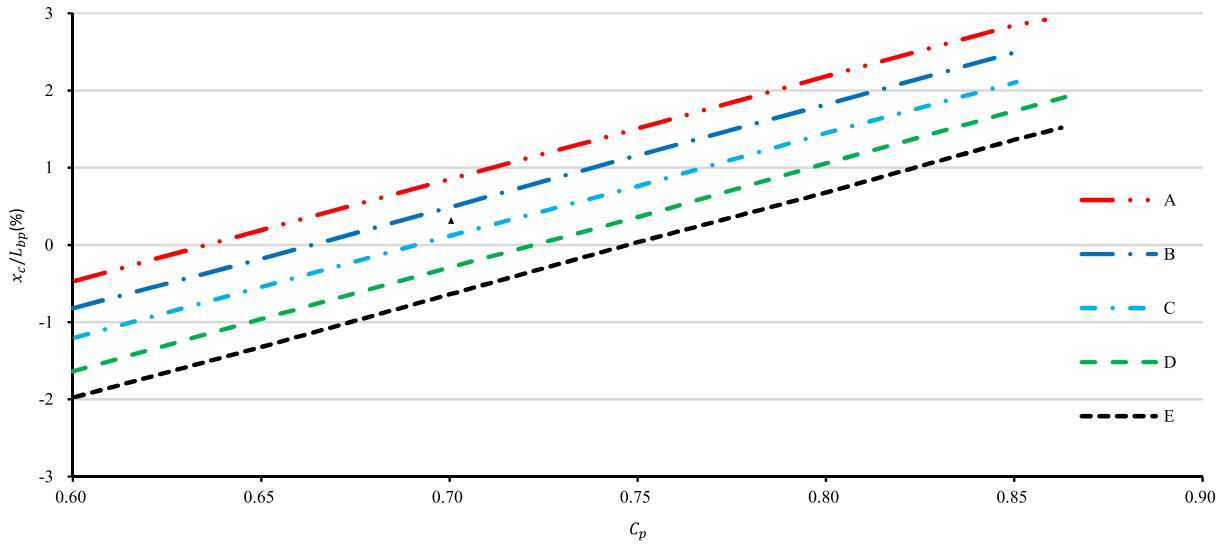
FIGURE 1. Selection of calculation map.

increase in fuel consumption. In the calculation of hydrostatic resistance R_{total}, the total hydrostatic resistance of the ship is composed of frictional resistance R_f and residual resistance R_r.

$$C_f = \frac{0.4621}{\lg Re^{2.6}} \tag{1}$$

$$Re = \frac{v_1 L_{WL}}{9.224 \times 10^{-7}} \tag{2}$$

$$\Delta C_f = [105 \times (\frac{K_s}{L_{WL}})^{\frac{1}{3}} - 0.64] \times 10^{-3} \tag{3}$$

$$R_f = \frac{\rho V_1^2 S(\Delta C_f + C_f)}{2000} \tag{4}$$

The remaining resistance (R_r) needs to be obtained through a series of calculations. The calculation model of R_r is given by Eq.(19). Initially, give some variables that need to be calculated. We need to determine whether the length modification is needed based on the value of L_{WL}/B. We need to determine whether the length modification is needed based on the value of L_{WL}/B. If the value is equal to 6.5, length and width correction is not required; otherwise, length and width correction is required [17].

$$\alpha = 0.674 \times \sin(L_{WL} \times 0.024 + 2.559)$$
$$+ 0.1644 \times \sin(L_{WL} \times 0.09254 - 2.719) \tag{5}$$

$$\xi = 557.1801 - 134.06849 \times g - 3.31675 \times g^2$$
$$+ 2.71624 \times g^3 - 0.16318 \times g^4 \tag{6}$$

The residual resistance correction factor α and the length and width correction percentage ξ are given by Eq.(5) and Eq.(6) respectively.

The residual resistance coefficient C_r is read from the map data. The five calculation graph formulas are shown Eq.(7) to Eq.(11).

$$A = 13.496 \times C_p - 8.4998 - L_{bp} \tag{7}$$

$$B = 13.28212 \times C_p - 8.81098 - L_{bp} \tag{8}$$

$$C = 13.23043 \times C_p - 9.15623 - L_{bp} \tag{9}$$

$$D = 13.51808 \times C_p - 9.77031 - L_{bp} \tag{10}$$

$$E = 13.32314 \times C_p - 9.98179 - L_{bp} \tag{11}$$

Figure 1 presents the schematic diagram of five curves. If given C_P of the ship, two adjacent ordinates y_a, y_b can be obtained in the selected calculation map to obtain the remaining resistance coefficient. The remaining resistance is obtained according to the remaining resistance coefficient. If C_P can be read directly on the map, the resistance value can be obtained according to the correction curve. When C_P is not on the curve, interpolation is needed for calculation.

The interpolation graph is shown in Figure 2. In actual operation, we convert five kinds of graphs into five data files. According to the five formulas A, B, C, D and E, if the data calculated by A is smaller than B, C, D and E, then we select the data file converted by A as the file for interpolation calculation [18]. The difference between the two calculation results is d. The interpolation calculation formula is shown by Eq.(12) to Eq.(17).

$$x = \frac{V_1}{\sqrt{C_P L_{WL}}} \tag{12}$$

$$C_m = \frac{C_b}{C_p} \tag{13}$$

$$A_m = C_m \times B \times T1 \tag{14}$$

$$C_r a = \frac{y_a A_m}{S} \times 10^{-3} \tag{15}$$

$$C_r b = \frac{y_b A_m}{S} \times 10^{-3} \tag{16}$$

$$C_R = C_r a + (C_r b - C_r a) \times d \tag{17}$$

From the variables obtained above, the formula of C_r can be obtained by Eq.(18), and we can also get the formula for
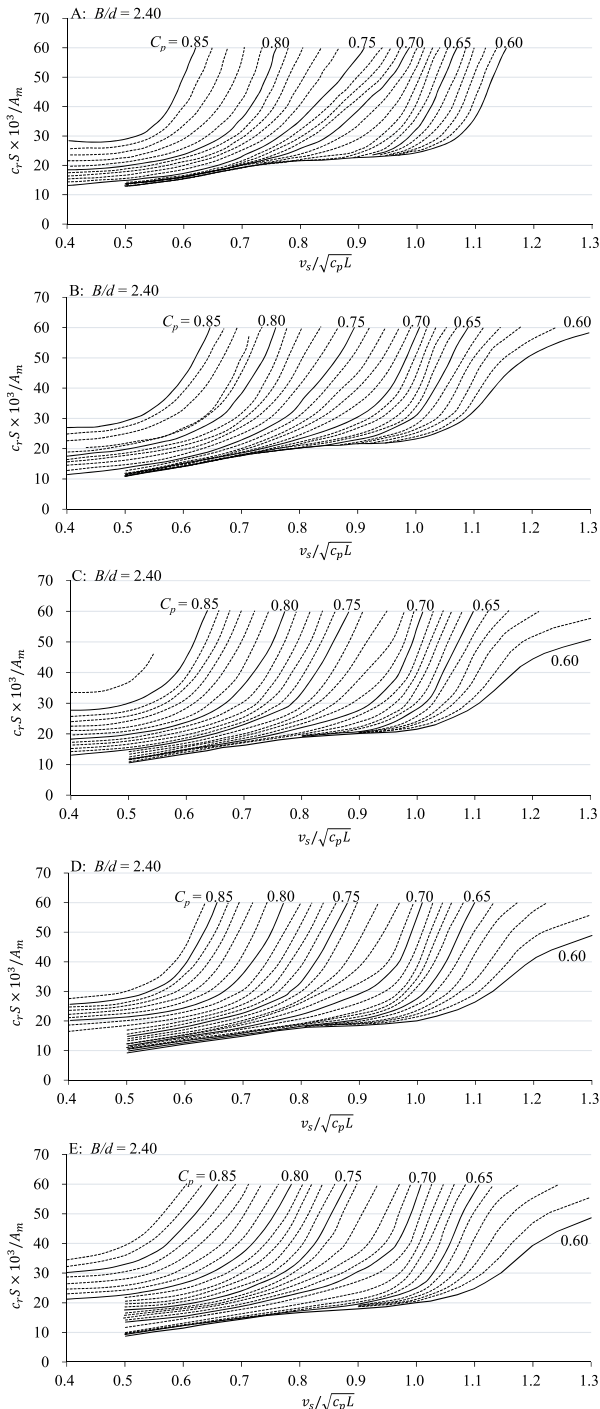
FIGURE 2. Five calculation maps.

TABLE 2. The stall direction factor C_β.

Wind and wave direction	Wind wave direction angle	C_β
Against the wind and wave	$0° \sim 30°$	$2C_\beta = 2$
Stem oblique wave and Front upwind	$30° \sim 60°$	$2C_\beta = 1.7 - 0.03(BN - 4)$
Beam sea and crosswind	$60° \sim 150°$	$2C_\beta = 0.9 - 0.06(BN - 6)$
Following sea and wind	$150° \sim 180°$	$2C_\beta = 0.4 - 0.03(BN - 8)$

TABLE 3. The stall size factor C_μ.

Square factor C_β	Loading situation	The stall size factor C_μ
0.55	common	$1.7 - 1.4F_r - 7.4F_r^2$
0.60	common	$2.2 - 2.5F_r - 9.5F_r^2$
0.65	common	$2.6 - 3.7F_r - 11.6F_r^2$
0.70	common	$3.1 - 5.3F_r - 12.4F_r^2$
0.75	common/full load	$2.4 - 10.6F_r - 9.5F_r^2$
0.80	common/full load	$2.6 - 13.1F_r - 15.1F_r^2$
0.85	common/full load	$3.1 - 18.7F_r + 28.0F_r^2$
0.75	ballast	$2.6 - 16.3F_r - 21.6F_r^2$
0.80	ballast	$3.0 - 16.3F_r - 21.6F_r^2$
0.85	ballast	$3.4 - 20.9F_r + 31.8F_r^2$

resistance R_{total1}.

$$R_{total1} = \frac{[C_f + \Delta C_f + (\frac{\Xi}{100} + 1)\alpha C_r]\rho V_1^2 S}{2000} \quad (20)$$

B. SPEED LOSS OF SHIP

Except the R_{total1}, the total additional resistance is another major factor that causes the ship's total resistance to sail at sea due to marine weather [19]. The effects of waves and wind are mainly discussed here. Therefore, the approximate method established by Kwon is used to estimate the impact of waves and wind [20]. Kwon method is shown by Eq.(21) to Eq.(24). Figure 3 presents the wind direction angle in the Kwon method.

$$F_r = \frac{V_1}{\sqrt{gL_{pp}}} \quad (21)$$

$$\frac{\Delta V}{V_1} = \frac{C_\beta C_\mu C_F}{100} \quad (22)$$

$$\Delta V = V_1 - V_{ship} \quad (23)$$

$$g = 9.8(\frac{m}{s^2}) \quad (24)$$

Here, C_β is the stall direction factor. It is related to the wind direction and the Beaufort Wind Scale, C_μ is the stall size factor, which varies with the square coefficient of the ship, the load, and the Fourud number, C_F is the factor of ship type, which related to the type of ship, Beaufort Wind Scale, and the displacement of the ship, V_{ship} is the vessel speed in current marine weather.

Table 2, Table 3 and Table 4 show the calculation formulas of C_β, C_μ and C_F under different constraints, respectively.

C. SHIP HOST POWER CALCULATION

The fuel consumption of a ship is closely related to the power of the main engine (P_e). Therefore, a calculation model of the host power needs to be given [4]. The main engine power is
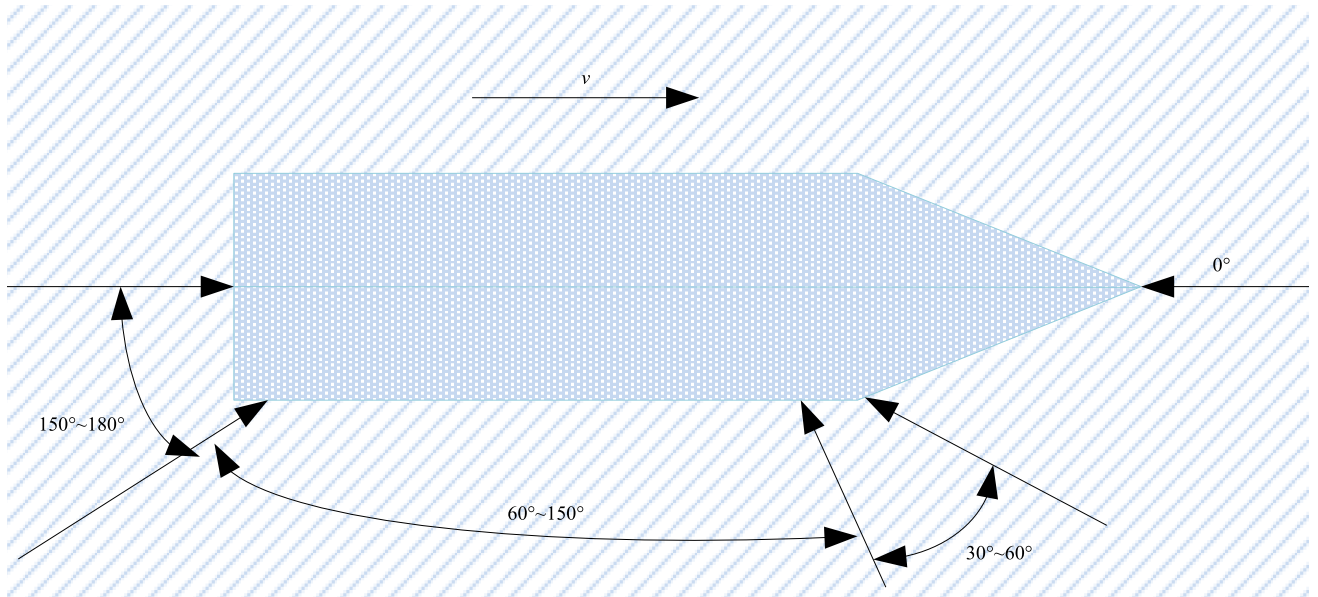
calculating total water resistance (R_{total1}) in Eq.(20).

$$C_r = \frac{C_R A_m d}{1000S} \quad (18)$$

$$R_r = \frac{(\frac{\Xi}{100} + 1)\alpha C_r \rho V_1^2 S}{2000} \quad (19)$$

After sorting and simplifying the formulas R_f and R_r, we can get the formula for calculating the total static water

FIGURE 3. Wind direction angle in Kwon method.

TABLE 4. The stall size factor C_F.

Ship type	Ship factor C_F
all ship types (except container ships) fully loaded	$0.5B_N + \frac{B_N^{6.5}}{2.7P^{2/3}}$
all ship types (except container ships) ballast status	$0.5B_N + \frac{B_N^{6.5}}{2.7P^{2/3}}$
container ship normal loading status	$0.7B_N + \frac{B_N^{6.5}}{2.2P^{2/3}}$

obtained by total resistance, ship speed and other parameters. The main engine power is also composed of the still water main engine power (P_{e1}) and the additional power (ΔP_e). The calculation for P_{e1} and ΔP_e are given by Eq.(25) to Eq.(31).

$$P_{d1} = \frac{R_{total1}V_1}{\eta_0} \tag{25}$$

$$P_{e1} = \frac{P_{d1}}{\eta_s} \tag{26}$$

$$R_{total2} = \frac{[C_f + \Delta C_f + (\frac{\Xi}{100} + 1)\alpha C_r]\rho V_{ship}^2 S}{2000} \tag{27}$$

$$\Delta R_{total} = R_{total1} - R_{total2} \tag{28}$$

$$\Delta P_d = \frac{\Delta R_{total}\Delta V_1}{\eta_0} \tag{29}$$

$$\Delta P_e = \frac{\Delta P_d}{\eta_s} \tag{30}$$

$$P_e = P_{e1} + \Delta P_e \tag{31}$$

D. FUEL CONSUMPTION

Through the above calculation of resistance and power, a model of fuel consumption can be obtained, which is the required objective function [21].

$$\begin{aligned} sfoc = {} & 0.20198 - 1.06628 \times 10^{-5} \times P_e + 1.59045 \times 10^{-9} \\ & \times P_e^2 - 1.35961 \times 10^{-13} \times P_e^3 \\ & + 5.67084 \times 10^{-18} \times P_e^4 \end{aligned} \tag{32}$$

The value of *sfoc* in Eq.(32) is the fuel consumption rate (kg/kw.h), and P_e in Eq.(31) is the power of the host (Kw). So, the fuel consumption *spef* is given by Eq.(33).

$$spef = sfoc \times P_e \tag{33}$$

Assuming the voyage is divided into K, given the coordinates of the starting point (x_1, y_1) and the next point(x_2, y_2), the distance (D_i) between the two points can be obtained by Eq.(34), and the time for voyage can be obtained according to the distance (D) in Eq.(35) and each speed in Eq.(36), the total fuel consumption of the route (F) in Eq.(39) can be obtained from each sailing time and fuel consumption per hour.

$$D_i = \frac{\arccos \sin y_1 \sin y_2 + \cos y_1 \cos y_2 \cos x_2 - x_1}{\Pi \times 180 \times 60} \tag{34}$$

$$D = \sum_{i=1}^{K} D_i \tag{35}$$

$$t_i = \frac{D_i}{3600V_{ship}} \tag{36}$$

$$T = \sum_{i=1}^{K} t_i \tag{37}$$

$$F_i = \frac{spef \ t_i}{1000} \tag{38}$$

$$F = \sum_{i=1}^{K} F_i \tag{39}$$

In summary, the objective function (F) of the ship sailing in marine weather is obtained by Eq.(39). Next, the mentioned whale optimization algorithm is used to optimize the objective function to obtain the desired fuel consumption.
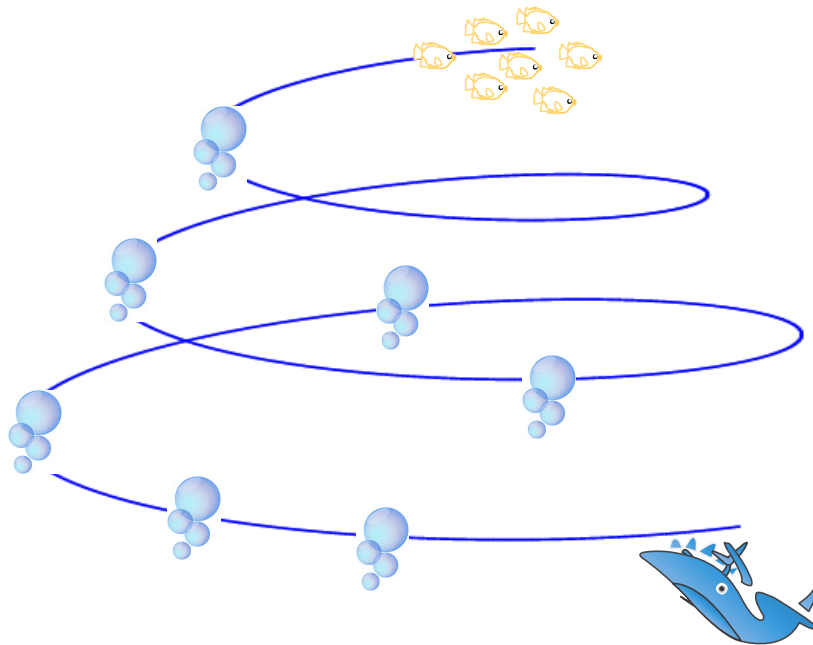
FIGURE 4. Bubble-net feeding behavior of humpback whales.

III. WHALE OPTIMIZATION ALGORITHM

Whales usually live in groups, and in the process of predation, they surround prey (fish and shrimp) on the surface of the sea and spit out spiral-shaped bubbles to prey. This predation behavior is called bubble predation. The bubble predatory method is specifically that the whale first dives into the water at a depth of about 15 meters and moves upwards in a spiral posture toward the water surface. During the swimming process, many bubbles of different sizes are spit out, so that the last spit and the first spit at the same time. It rises to the surface of the water, simultaneously, the spit air bubbles form a cylindrical or tubular bubble web, like a web woven by a spider, which encloses the prey tightly and presses towards the center of the web. Then, the whale opens the mouth almost upright in the bubble circle and swallowed the prey in the net. The bubble predation behavior is shown in Figure 4 [22].

Inspired by this special predator behavior, the swarm intelligence optimization algorithm WOA simulates the predation behavior of whales in the ocean, and achieves the purpose of optimizing search by whale enveloping and bubble attacking prey [23]. Consistent with the classic particle swarm algorithm, ant colony algorithm [24], and artificial bee colony algorithm, the essence is the process of statistical optimization. Because of its advantages of simple operation, few parameters, and excellent performance, the WOA has received extensive attention from many scholars, and it has been applied to different practical problems [25].

A. MATHEMATICAL MODEL OF WHALE OPTIMIZATION ALGORITHM

The whale optimization algorithm includes three main stages: random search for food, surround predation and bubble

predation. Assume that the size of the whale population is N and the dimension of the problem space is D. Then the position of the i-th whale in D-dimensional space is $X_i = (x_1^1, x_2^2, \ldots, x_N^D, i = 1 \; to \; N)$, and the position of the optimal whale (predatory prey) corresponds to the global optimal solution.

1) WHALE PREDATION

During the predation process, the whale first observes the location of the prey and then surrounds it. In the whale algorithm, it is assumed the solution and the problem variables are also the position of the lead whale (prey). After defining the position of the best whale, other whale will swim towards the position of the whale to update its position. In contrast, the distance between the individual and the optimal whale position (prey) needs to be solved based on Eq.(40) in the WOA.

$$\vec{D} = |\vec{C}\vec{X}^*(t) - \vec{X}(t)| \tag{40}$$

where $\vec{X}^*(t)$ represents the position of the best whale in the t generation (position of prey), $\vec{X}(t)$ represents the the position of the whale in the t generation, $\vec{X}^*(t)$ updates its position with each iteration, and constant $\vec{C}$ is the swing factor in Eq.(40).

The whale is updated according to the position of the lead whale. The position update formula is given by Eq.(41) to Eq.(43).

$$\vec{X}^*(t+1) = \vec{X}^*(t) - \vec{A}\vec{D} \tag{41}$$

$$\vec{C} = 2\vec{r} \tag{42}$$

$$\vec{A} = 2\vec{a}\vec{r} - \vec{a} \tag{43}$$

where $\vec{r}$ is a random number between [1, 0], and $\vec{a}$ decreases linearly from 2 to 0, as the number of iterations increases.

2) BUBBLE PREDATOR BY WHALE(LOCAL SEARCH PHASE)

To simulate the bubble predation behavior of a whale, two strategies can be described as follows:

a: SWING SURROUNDED BY PREDATOR

The position of the whale at this stage is obtained by updating. The convergence factor $\vec{A}$ at this stage is achieved with a linear decrease of α from 2 to 0. A is a random value between $[-\alpha, \alpha]$. When the random value A is between $[-1,1]$, the next position of the whale may be any position between the current position of the whale and the position of the prey.

b: SPIRAL BUBBLE PREDATOR

At this stage, the whale first calculates the distance between itself and its prey (the best position so far), and then the whale moves upstream in a spiral posture and spit out bubbles of varying sizes to hunt fish and shrimp. The mathematical model of this behavior is given by Eq.(44) to Eq.(45).

$$\vec{D}' = |\vec{X}^*(t) - \vec{X}(t)| \tag{44}$$

$$\vec{X}'(t+1) = \vec{D}'\varrho^{bl}\cos(2\Pi l) + \vec{X}^*(t) \tag{45}$$

where $\vec{D}'$ is the distance from the i-th whale to the food, l is a random value between $[-1,1]$, and b is a spiral constant.

In the process of whale predation, there are two mechanisms: sway encircling predation and bubble predation. Therefore, it is assumed that the probability that the whale performs two predatory behaviors is 50%, that is, the whale updates its position every time with 50% probability.The mathematical model is given by Eq.(46):

$$\vec{X}(t+1) = \begin{cases} \vec{X}^*(t) - \vec{A}\vec{D}, & \text{if } p < 0.5 \\ \vec{D}'\varrho^{bl}\cos(2\Pi l) + \vec{X}^*(t), & \text{if } p \geq 0.5 \end{cases} \tag{46}$$

3) WHALE SEARCHING FOR PREY RANDOMLY(GLOBAL SEARCH PHASE)

Researchers have discovered that during the predation process, the whale will follow its partner's position and change to update its position. In other words, the whale at this stage will no longer update its position following the position of the best whale, but it will perform a random large-scale search for prey to determine the next position where needed to update. Therefore, in this algorithm, the whale performs a larger range search at this stage according to the change of the value of the convergence factor $|\vec{A}|$. When $|\vec{A}| > 1$, the whale will perform a random search for prey and perform a global search to avoid falling into a local optimum. The mathematical formula at this stage is presents by Eq.(47) to Eq.(48)

$$\vec{D} = |\vec{C}\vec{X}_{rand}(t) - \vec{X}(t)| \tag{47}$$

$$\vec{X}(t+1) = \vec{X}_{rand}(t) - \vec{A}\vec{D} \tag{48}$$

where $\vec{X}_{rand}$ is the position of a random whale (or prey) in the current population.

This section details the basic principles and mathematical models of the whale optimization algorithm. In the following
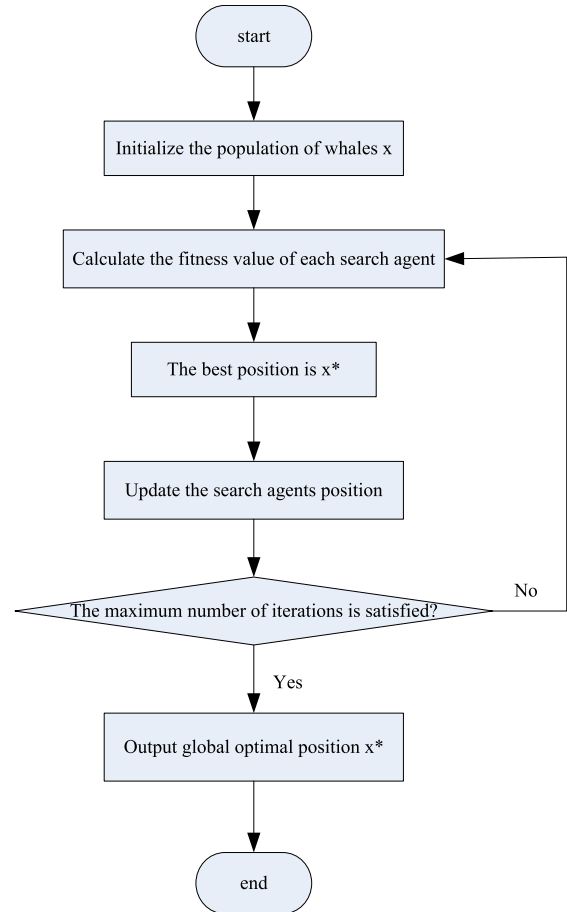

FIGURE 5. The flow chart of WOA.

subsection B, we discuss the whale optimization algorithm in detail to solve route planning under complex marine weather.

B. ALGORITHM WOA FOR SHIP PATH PLANNING

The whale optimization algorithm is applied to the ship path planning problem. The optimization space of the algorithm represents the ship path optimization space. Each whale represents a route from the starting point to the end point. The mathematical model of the ship path planning is the objective function of the whale optimization algorithm [22]. A good whale position represents the best path, and the flow chart is given by Figure 5.

IV. SIMULATION EXPERIMENTS

A. SIMULATION PLATFORM

The test environment is set up on a computer with Intel Core i5-6500 CPU, 3.20 GHz, 8GB RAM, running on Windows 7.

B. EXPERIMENTAL SETUP

In this section, WOA is benchmarked in two simulation cases.In the first case, it is a route from Tokyo to Oakland, where the starting point and the terminal point described by latitude and longitude are (35,139) and (38,-127) respectively. Similarly, the starting point and the terminal point of the route from Keelung to Rabaul in the second case are (25,121) and
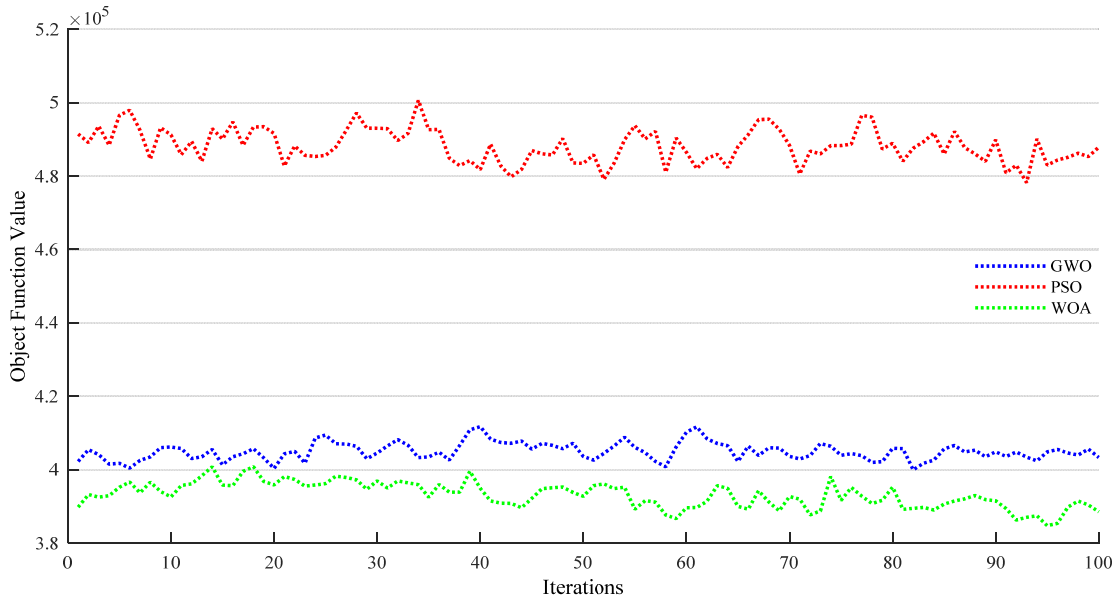
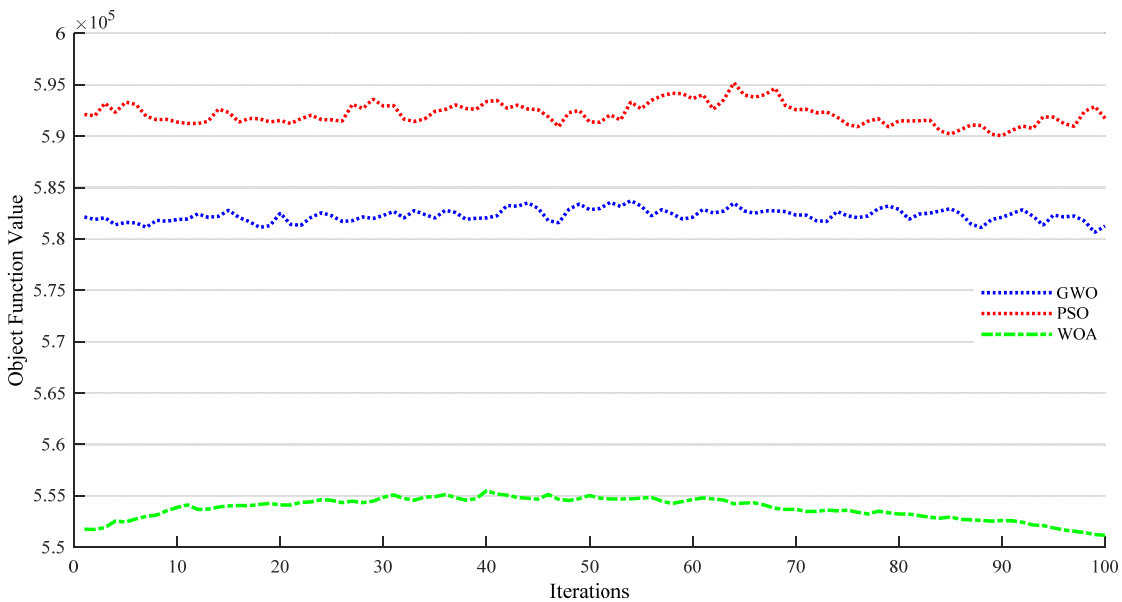**FIGURE 6.** The convergence curves for case 1.

FIGURE 7. The convergence curves for case 2.

(4,152) respectively. These latitudes and longitudes are integerized for calculation. To verify our method, we compared the WOA with PSO and GWO, the corresponding parameters of which are given in Table 5. Such values represent the best parameter sets for these algorithms. In all the three experiments, the swarm population is 30 and the maximum iteration number is set to 100.

TABLE 5. The initial parameters of algorithms.

Algorithm	Parameter	value
WOA	$\vec{a}$	linearly decreased from 2 to 0
GWO	$\vec{a}$	linearly decreased from 2 to 0
PSO	Cognitive constant (C_1)	1.5
	Social constant (C_2)	2
	Inertia constant (ω)	1

C. EXPERIMENTAL RESULTS AND ANALYSIS

The experimental results are shown in Table 6. In the table, Best, Worst, Mean, and Std represent the best fitness value, the worst fitness value, the average fitness value, and the standard deviation, respectively. The best results are denoted in bold type. The results are averaged over 30 independent runs. It is clearly that, to settle the minimum fuel consumption problem of route planning, the performance of WOA is better than PSO and GWO. The best fitness value of WOA is lower
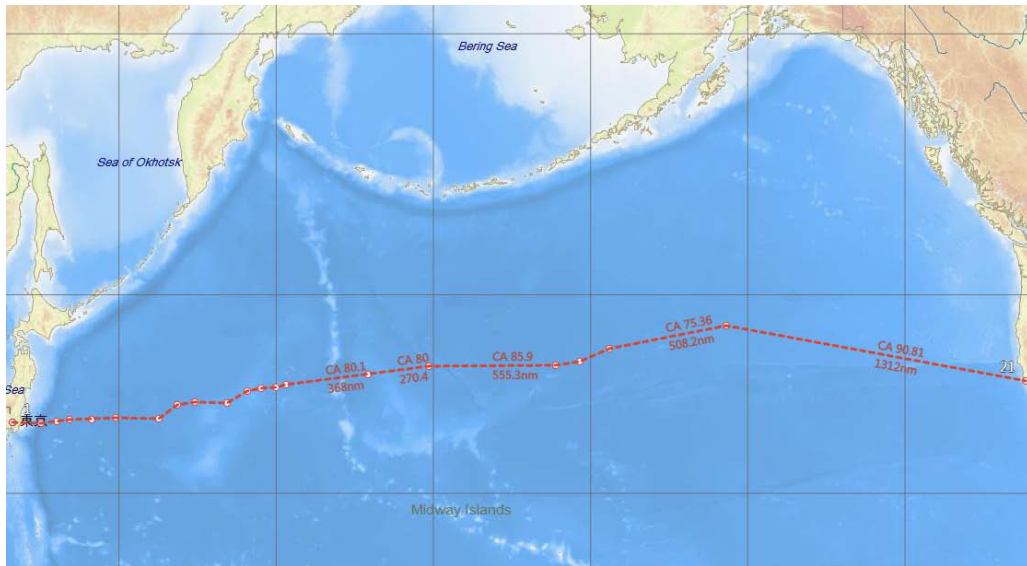
FIGURE 8. The actual route for case 1.

FIGURE 9. The actual route for case 2.

than the competing algorithms, which indicates that the WOA is more suitable for such route planning. In the comparison of the test results of the three algorithms, the variance value of the GWO is the smallest, indicating that the test results which produced by the algorithm running independently for 30 times have little fluctuation. Figures 6 and Figure 7 show the convergence of the three algorithms. The convergence curve is the result of 30 independent runs of the three algorithms, where all the convergence curves are drawn as mean values.

It can be obtained from the convergence curve that the convergence performance of the WOA is better than the other two algorithms. The objective function value obtained by the

WOA is always lower than the other two algorithms. It can be concluded that the WOA has a strong approximation ability of the optimal value.

According to the experimental results of the algorithm operation, the actual routes of the two cases obtained through simulation are shown in Figure 8 and Figure 9.

The variance reflects the stability of the algorithm. Figures 10 and Figures 11 show the variance diagram of the three algorithms.The smaller the variance, the smaller the data fluctuation. In the case 1, the variance of the PSO is the smallest. But in the case 2, the variance of the WOA is the smallest.
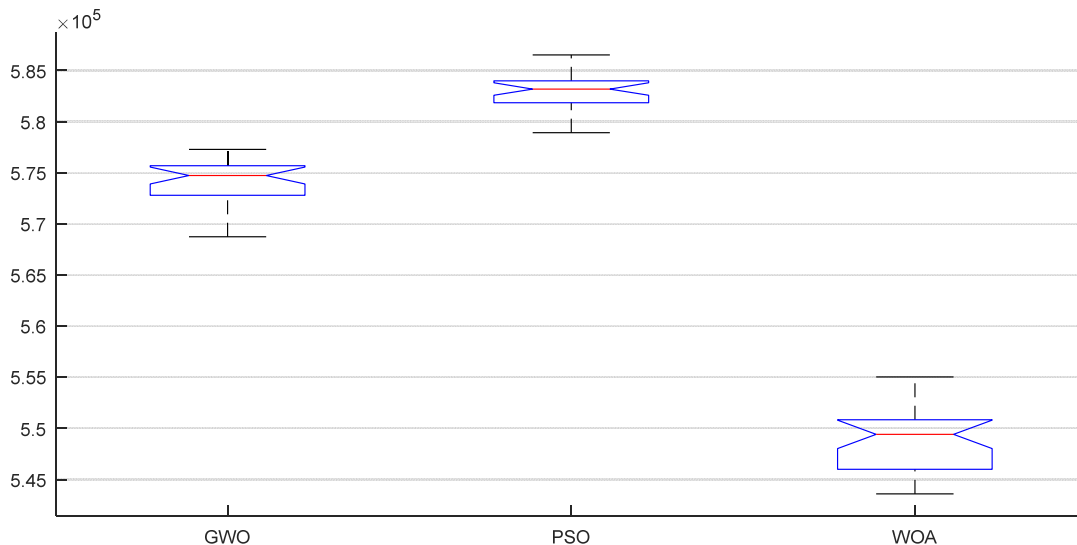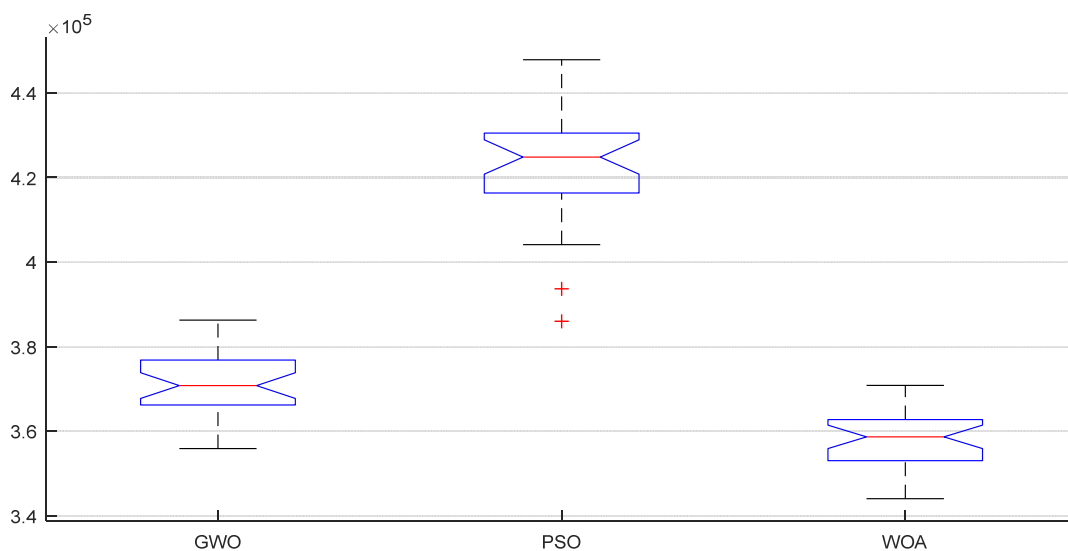
FIGURE 10. The variance diagram for case 1.

FIGURE 11. The variance diagram for case 2.

TABLE 6. Experimental results for the two test case.

Start/end Point	Result	GWO	PSO	WOA
$(38, 139), (35, -127)$	Best	568.745	578.925	**543.597**
	Worst	577.813	586.631	**555.044**
	Mean	574.215	582.667	**548.937**
	Std	2.130	**1.856**	3.231
$(25, 121), (4, 152)$	Best	355.891	385.986	**344.015**
	Worst	386.268	447.861	**370.805**
	Mean	372.226	423.078	**358.317**
	Std	7.424	13.479	**6.268**

TABLE 7. p-value Wicoxon rank-sum test.

Expeimentst	WOA vs. PSO	WOA vs. WOA
Case 1	$3.0109 \times e^{-11}$	$2.3897 \times e^{-8}$
Case 2	$3.0213 \times e^{-11}$	$2.9784 \times e^{-8}$

In summary, it can be concluded that fuel consumption is very important in the problem of ship path planning. When using a population-based algorithm to solve ship routing problems, low fuel consumption is our goal. This study shows that WOA is very suitable for solving this problem.

V. CONCLUSIONS AND FUTURE WORKS
In this paper, the WOA is used to find the optimal path for the ship path planning problem under the complicated large amount of marine meteorological. The high exploration and development of this algorithm is the motivation of this paper.

In order to verify the validity of the test results, a *p*-value Wicoxon rank-sum test is performed in Table 7. $p > 0.05$ indicates that there is no significant difference between the algorithms, and $p < 0.05$ indicates that there is a significant difference. The data is not obtained by accident and has reference value.

The algorithm is applied to two test cases. For verification, the results of WOA are compared with two stochastic optimization algorithms of PSO and GWO. The results show that this method can effectively solve the problem of ship path planning. Because the WOA has a very high local optimal avoidance, which increases the probability of finding the optimal weighting of the path and the appropriate approximation of the cost. In addition, due to the high exploitation of WOA, the accuracy of the weighted and cost optimal values obtained is very high. The next work will focus on these two issues. On the one hand, WOA will be used to solve the problem of ships avoiding obstacles such as islands and shallow waters. On the other hand, we will try to use other better algorithms to solve the same problem.

REFERENCES

[1] A. Alvarez, A. Caiti, and R. Onken, "Evolutionary path planning for autonomous underwater vehicles in a variable ocean," *IEEE J. Ocean. Eng.*, vol. 29, no. 2, pp. 418–429, Apr. 2004.

[2] R. Song, Y. Liu, and R. Bucknall, "A multi-layered fast marching method for unmanned surface vehicle path planning in a time-variant maritime environment," *Ocean Eng.*, vol. 129, pp. 301–317, Jan. 2017.

[3] Y. Liu and R. Bucknall, "Path planning algorithm for unmanned surface vehicle formations in a practical maritime environment," *Ocean Eng.*, vol. 97, pp. 126–144, Mar. 2015.

[4] B. Yoo and J. Kim, "Path optimization for marine vehicles in ocean currents using reinforcement learning," *J. Mar. Sci. Technol.*, vol. 21, no. 2, pp. 334–343, Jun. 2016.

[5] J. Xin, J. Zhong, S. Li, J. Sheng, and Y. Cui, "Greedy mechanism based particle swarm optimization for path planning problem of an unmanned surface vehicle," *Sensors*, vol. 19, no. 21, p. 4620, 2019.

[6] D. Wei, F. Wang, and H. Ma, "Autonomous path planning of AUV in large-scale complex marine environment based on swarm hyper-heuristic algorithm," *Appl. Sci.*, vol. 9, no. 13, p. 2654, 2019.

[7] H. He, J. Zheng, F. Yu, L. Yu, and E. Zhan, "Exoskeleton robot gait detection based on improved whale optimization algorithm," *J. Comput. Appl.*, vol. 39, no. 7, pp. 1905–1911, 2019.

[8] H. Zhou, Z. Zeng, and L. Lian, "Adaptive re-planning of AUVs for environmental sampling missions: A fuzzy decision support system based on multi-objective particle swarm optimization," *Int. J. Fuzzy Syst.*, vol. 20, no. 8, pp. 650–671, Oct. 2017.

[9] K. Opara and J. Arabas, "Comparison of mutation strategies in differential evolution—A probabilistic perspective," *Swarm Evol. Comput.*, vol. 39, pp. 53–69, Apr. 2018.

[10] Y. Wang, H. Chen, and H. Li, "3D path planning approach based on gravitational search algorithm for sprayer UAV," *Trans. Chin. Soc. Agricult. Mach.*, vol. 49, pp. 28–33, Feb. 2018.

[11] Y.-N. Ma, Y.-J. Gong, C.-F. Xiao, Y. Gao, and J. Zhang, "Path planning for autonomous underwater vehicles: An ant colony algorithm incorporating alarm pheromone," *IEEE Trans. Veh. Technol.* vol. 68, no. 1, pp. 141–154, Jan. 2019.

[12] A. Zamuda, J. D. Hernández Sosa, and L. Adler, "Constrained differential evolution optimization for underwater glider path planning in submesoscale eddy sampling," *Appl. Soft Comput.*, vol. 42, pp. 93–118, May 2016.

[13] Y. Zhou and R. Wang, "An improved flower pollination algorithm for optimal unmanned undersea vehicle path planning problem," *Int. J. Pattern Recognit. Artif. Intell.*, vol. 30, no. 4, May 2016, Art. no. 1659010.

[14] R. K. Dewangan, A. Shukla, and W. W. Godfrey, "Three dimensional path planning using grey wolf optimizer for UAVs," *Applied Intelligence*, vol. 49, no. 6, pp. 2201–2217, Jun. 2019.

[15] K. Tziortziotis, N. Tziortziotis, K. Vlachos, and K. Blekas, "Motion planning with energy reduction for a floating robotic platform under disturbances and measurement noise using reinforcement learning," *Int. J. Artif. Intell. Tools*, vol. 27, no. 4, Jun. 2018, Art. no. 1860005.

[16] Y.-H. Lin, L.-C. Huang, S.-Y. Chen, and C.-M. Yu, "The optimal route planning for inspection task of autonomous underwater vehicle composed of MOPSO-based dynamic routing algorithm in currents," *Appl. Ocean Res.*, vol. 75, pp. 178–192, Jun. 2018.

[17] H. N. Psaraftis and C. A. Kontovas, "Ship speed optimization: Concepts, models and combined speed-routing scenarios," *Transp. Res. C, Emerg. Technol.*, vol. 44, pp. 52–69, Jul. 2014.

[18] C. Maxted and W. Waller, "Development of an intelligent controller for power generators," *J. Phys., Conf. Ser.*, vol. 15, pp. 306–310, Jan. 2005.

[19] K. Blekas and K. Vlachos, "RL-based path planning for an over-actuated floating vehicle under disturbances," *Robot. Auto. Syst.*, vol. 101, pp. 93–102, Mar. 2018.

[20] D. A. Bainbridge, "Buried clay pot irrigation: A little known but very efficient traditional method of irrigation," *Agricult. Water Manage.*, vol. 48, no. 2, pp. 79–88, Jun. 2001.

[21] T. Dickson, H. Farr, D. Sear, and J. I. R. Blake, "Uncertainty in marine weather routing," *Appl. Ocean Res.*, vol. 88, pp. 138–146, Jul. 2019.

[22] T.-K. Dao, T.-S. Pan, and J.-S. Pan, "A multi-objective optimal mobile robot path planning based on whale optimization algorithm," in *Proc. IEEE 13th Int. Conf. Signal Process. (ICSP)*, Nov. 2016, pp. 337–342.

[23] A. G. Hussien, E. H. Houssein, and A. E. Hassanien, "A binary whale optimization algorithm with hyperbolic tangent fitness function for feature selection," in *Proc. 8th Int. Conf. Intell. Comput. Inf. Syst. (ICICIS)*, Dec. 2017, pp. 166–172.

[24] L. Yue and H. Chen, "Unmanned vehicle path planning using a novel ant colony algorithm," *EURASIP J. Wireless Commun. Netw.*, vol. 2019, no. 1, Dec. 2019, Art. no. 136.

[25] B. Bentouati, L. Chaib, and S. Chettih, "A hybrid whale algorithm and pattern search technique for optimal power flow problem," in *Proc. 8th Int. Conf. Modeling, Identificat. Control (ICMIC)*, Nov. 2016, pp. 1048–1053.

[26] X. Yu, W.-N. Chen, T. Gu, H. Yuan, H. Zhang, and J. Zhang, "ACO-A*: Ant colony optimization plus A* for 3-D traveling in environments with dense obstacles," *IEEE Trans. Evol. Comput.*, vol. 23, no. 4, pp. 617–631, Aug. 2019.

[27] Z. Chen, Y. Zhang, Y. Zhang, Y. Nie, J. Tang, and S. Zhu, "A hybrid path planning algorithm for unmanned surface vehicles in complex environment with dynamic obstacles," *IEEE Access*, vol. 7, pp. 126439–126449, 2019.

[28] H. Wang, F. Guo, H. Yao, S. He, and X. Xu, "Collision avoidance planning method of USV based on improved ant colony optimization algorithm," *IEEE Access*, vol. 7, pp. 52964–52975, 2019.

QILONG HAN is currently a Professor and the Deputy Dean of the College of Computer Science and Technology, Harbin Engineering University. His research interests include data security and privacy, mobile computing, and distributed and networked systems. He has more than 60 publications as edited books and proceedings, invited book chapters, and technical articles in refereed journals and conferences. He is a Senior Member of CCF and the Chair of CCF YOCSEF Harbin. He has served as the Program Committee Member and the Co-Chair for a number of international conferences/workshops for areas, including web intelligence, e-commerce, data mining, intelligent systems, and so on.

XIAO YANG received the B.Eng. degree from Guangxi University for Nationalities, China, in 2018. He is currently pursuing the Ph.D. degree with Harbin Engineering University, China. His research interests include data mining, swarm intelligence algorithm, and machine learning.

HONGTAO SONG received the Ph.D. degree in automation from Harbin Engineering University, China, in 2009. He is currently an Assistant Professor with the College of Computer Science and Technology, Harbin Engineering University, China. His research interests include sensor networks, machine learning, and the IoT.

HUI ZHANG received the bachelor's and Graduate degrees from the Harbin University of Engineering, in 2019. She is currently pursuing the master's degree with the College of Computer Science and Technology. Her main research interests include data mining and machine learning.

SHANSHAN SUI received the bachelor's degree in computer science and technology from Northeastern University. She is currently pursuing the master's degree in software engineering with Harbin Engineering University. Her main research interests include data mining and deep learning.

ZAIQIANG YANG received the bachelor's degree in information management from the Central Judicial Police Academy. He is currently pursuing the master's degree in computer science and technology with Harbin Engineering University. His main research interests include data mining and deep learning.

• • •